C.P. No. 443
(20,720)
A.R.C. Technical Report

C.P. No. 443
(20,720)
A.R.C. Technical Report

MINISTRY OF SUPPLY

AERONAUTICAL RESEARCH COUNCIL

CURRENT PAPERS

Shock Speed and Running Time Measurements in the N.P.L. Hypersonic Shock Tunnel

by

B. D. Henshall, B.Sc., Ph.D.,
of the Aerodynamics Division, N.P.L.

LONDON: HER MAJESTY'S STATIONERY OFFICE

1959

FOUR SHILLINGS NET

C.P.No.443

Shock Speed and Running Time Measurements in the N.P.L. Hypersonic Shock Tunnel

- By -
K. D. Henshall, B.Sc., Ph.D.
of the Aerodynamics Division, N.P.L.

23rd January, 1959

SUMMARY

Resistance thermometers have been used in the measurement of shock speeds and running times in the N.P.L. Hypersonic Shock Tunnel. From an analysis of the first 600 runs, a method has been devised which enables the gasdynamic operation of the shock tunnel to be checked and any irregularities discovered.

---

1. Introduction

Some notes on the construction and instrumentation of the hypersonic shock tunnel at the National Physical Laboratory have been given in Refs. 1 and 2. The present report describes the initial experiments undertaken with this equipment and illustrates some difficulties which were encountered in the operation of the shock tunnel and in the evaluation of the results.

2. Experimental Details

A schematic diagram of the present arrangement of the N.P.L. hypersonic shock tunnel is given in Fig.1. The high pressure chamber is 2 ft 6 in. long, 3 in. internal and 8 in. external diameter stainless steel. At present the maximum operating pressure has been restricted to 130 atmospheres by available bottle storage pressure. In all runs to date the driving gas has been unheated hydrogen, and the driven gas has been undried air. The channel and intermediate chamber are constructed from mild steel 3 in. internal and 4 in. external diameter and are respectively 18 and 14 feet in length. Provision is made for six pairs of shock speed detector stations at positions along the channel denoted by A_1, A_2, B_1, B_2 ..... F_1, F_2. The distances of these stations from the main diaphragm are given in Fig.1. The nozzle has an expansion semi-angle of 11 degrees, 25 minutes, and is made of cast iron with replaceable mild steel nozzle lips at the inlet: the working section is $15\frac{1}{2}$ in. internal diameter and 8 feet in length. All detectors or transducers mounted in the working section are denoted by M_1 M_2 ..... for convenience.

After initial experiments[1] with "light screens"[4] as shock-wave detectors, it was decided to standardise resistance thermometers as our shock-wave detection equipment.

Two difficulties arise with the light screen technique: firstly, it is insensitive when low-channel pressures are used, and secondly the photomultiplier detects the radiation from ionised gas behind the shock wave before the shock wave passes the detector station. Some effort was directed to this problem by attempting better collimation of the light screen; however this technique was discarded in favour of the thin-film

resistance/

Published with permission of the Director, N.P.L.

resistance thermometer method. The procedure adopted at N.P.L. in the use of resistance thermometers for heat transfer work in shock tubes has been described in Ref.3, and our methods of construction, calibration and use will not be described in the present report.

Thus our experimental investigation of shock speeds down the channel of the shock tunnel began with four 'wall-type' thin-film resistance thermometers in the positions labelled A_2, B_2, E_2 and F_2 in Fig.1. One further 'stagnation-point-type' resistance thermometer was mounted in the expanded flow working section: this is denoted by W_S in the following discussion.

3. Runs 1 → 232

As the raw shock speed data was accumulated, it became increasingly obvious that either the shock wave was behaving in an erratic manner as it travelled down the channel of the shock tunnel, or the recording instrumentation was not functioning correctly. Moreover, a disquieting feature of the experiments was the variation in the shock speed over a given interval along the tube when the overall pressure ratio and downstream pressure in the channel were kept constant from run to run. Such unexpected results are well illustrated in Fig.2 where the shock Mach number $M_{S_{EF}}$ over the distance EF is plotted against the theoretical shock Mach number $M_{S_{TH}}$ corresponding to the initial pressure ratio across the diaphragm (see Ref.13 for the theoretical calculations). For example, at a diaphragm pressure ratio corresponding to a theoretical shock Mach number of 10.0, the measured shock Mach number $M_{S_{EF}}$ varied from 7.3 to 13.8! Furthermore, in most runs one or other of the resistance thermometer timing units failed to function. The very large experimental scatter observed in Fig.2 for measurements of the shock velocity over a distance EF(= 1 foot) were not observed when the average shock speed over a distance AF(= $19\frac{1}{8}$ feet) was compared to the theoretical shock speed as in Fig.3. However, considerable scatter is also present in Fig.4 where $M_{S_{AB}}$ is plotted against $M_{S_{TH}}$. Such results indicate strongly that the individual readings of shock speed over intervals of one foot (i.e., over AB and EF) must be suspect; whilst it is extremely likely that the gasdynamic operation of the shock tunnel is as predicted theoretically from the results for the much longer distance AF. These conclusions have since been substantiated by experiments described later in this report.

4. Runs 233 → 620

In Section 3 above, all experiments were carried out with 'uncalibrated' resistance thermometers. The method of calibration is fully described in Ref.3; here it is sufficient to note that the value of the calibration constant for an individual resistance thermometer should be within the range 0.02 to 0.07.

When the 5 resistance thermometers which had been used in all runs up to No. 232 were calibrated, it was found that two would not calibrate (that is, they became open-circuited during the calibration procedure) and one other had a calibration constant outside the acceptable range. Immediately it became clear that the most probable cause of our experimental difficulties was the use of uncalibrated resistance thermometers. All runs from No. 233 onwards have been made using calibrated wall and stagnation point resistance thermometers, and the improvement in the reproducability of results has been extraordinary. No reasonable explanation has been advanced to prove how or why uncalibrated gauges are so much inferior to models which have the 'correct' value of the calibration constant; it can merely be reported that this is so.

In/

In order to complete the investigation, an exhaustive check was made of the bandwidth, gain and response to input signals for each resistance thermometer trigger amplifier. No modifications were found necessary in the electronic performance of these units. A brief specification of these NPL-built units appears below and the corresponding circuit diagram appears as Fig.5. These units were designed for inputs of not less than 5 millivolts to ensure that the final thyratron output is triggered with negligible delay with respect to the input pulse. The gain of such trigger amplifiers is between 1000 and 3000 and typical bandwidth figures are

- 3dB at 11.5 Kc/s and 1 Mc/s, and

- 6dB at 6.5 Kc/s and 2 Mc/s.

The pulse response of the amplifier was checked using a 10 mV 1 μsec pulse from a pulse generator (Philips type GM 2314), and the output + ve and - ve trigger pulses were adjusted to be about 30 volts and of less than $\frac{1}{5}$ μsec rise time. Thus they are certain to operate counter chronometers correctly.

4.1 The output from resistance thermometers

From the many runs which have now been made using calibrated resistance thermometers we may derive a useful practical chart which illustrates the expected output from a resistance thermometer for a given shock Mach number. We may define two important quantities, ΔV_{JUMP} and ΔV_{MAX}. These quantities are illustrated schematically in Fig.6(a) for the two relevant cases of wall and stagnation point. Fig.6(b) shows two specimen experimental results of the series used in the preparation of Fig.7. It should be noted that Fig.7 will apply to all shock tube experiments using resistance thermometers made by painting[3] Hanovia 05 Liquid Bright Platinum on to glass models. If the standing voltage across the film is different from the 1 volt used in the N.P.L. experiments, the magnitudes of ΔV_{JUMP} and ΔV_{MAX} will be directly proportional to the value of standing voltage across the film.

The magnitude of ΔV_{JUMP} may be calculated from classical heat transfer theory - see, for example, Refs. 7 and 8. The instantaneous jump of surface temperature ΔT is approximately given by

$$\Delta T = (T_2 - T_1)\sqrt{\frac{(\rho cK)_2}{(\rho cK)_1}} \qquad \ldots(1)$$

where suffix $_2$ refers to the gas at high temperature and suffix $_1$ refers to the backing material of the thin film resistance thermometer (e.g., glass). ρ, c and K are respectively the density, specific heat and thermal conductivity of the gas or backing material. From the above relation it is clear that the magnitude of ΔT (and hence ΔV_{JUMP}) is directly proportional to the square root of the density of the hot gas behind the initial shock wave. Thus the experimental signals given in Fig.7 have been normalised to atmospheric density behind the incident shock wave. For each trace analysed, the density behind the shock has been calculated from the measured incident shock Mach number and the initial channel pressure. The observed signal ΔV_{JUMP} has been subsequently multiplied by the square root of the ratio of atmospheric density to the experimental density behind the shock. Now the jump in voltage ΔV_{JUMP} is related to the jump in temperature ΔT by

$$\Delta V = I_o \Delta R_o = I_o R_o \alpha \Delta T = V_o \alpha \Delta T$$

where α is the temperature coefficient of resistivity and V_o is the standing voltage across the film.

Now/

Now from (1) $$\frac{\Delta T}{T_1} = \left(\frac{T_2}{T_1} - 1\right)\sqrt{\frac{(\rho cK)_2}{(\rho cK)_1}}.$$

Thus, according to our approximate theory

$$\Delta V = V_o.\alpha.T_1\left(\frac{T_2}{T_1} - 1\right)\sqrt{\frac{(\rho cK)_2}{(\rho cK)_1}}. \qquad \ldots(2)$$

This equation may be rewritten as

$$\Delta V = V_o.\alpha.T_1\left(\frac{T_2}{T_1} - 1\right)\sqrt{\frac{\rho_2}{\rho_o}}\sqrt{\frac{c_2}{c_o}}\sqrt{\frac{K_2}{K_o}}\sqrt{\frac{\rho_o c_o K_o}{(\rho cK)_1}} \qquad \ldots(3)$$

where suffix $_o$ denotes atmospheric (room) conditions for air. The quantities $\frac{\rho_2}{\rho_o}$; $\frac{c_2}{c_o}$, $\frac{K_2}{K_o}$ and $\frac{T_2}{T_1}\left(=\frac{T_2}{T_o}\right)$ are known functions of the incident shock Mach number M_S and are available in tabular[11] and graphical[11,12] form. The value of $\sqrt{\rho_o c_o K_o}$ for room temperature air[9] is 1.12×10^{-4} and $\sqrt{(\rho cK)_1}$ for glass[9] is 0.031. We let $T_1 = T_o = 288°K$ and take[10] $\alpha = 0.00092$ per °K. Then if ΔV is measured in millivolts and V_o in volts we obtain, very nearly,

$$\frac{\Delta V}{V_o}\sqrt{\frac{\rho_o}{\rho_2}} = \sqrt{\frac{c_2}{c_o}}\sqrt{\frac{K_2}{K_o}}\left(\frac{T_2}{T_1} - 1\right). \qquad \ldots(4)$$

For the experimental data presented in Fig.7, the initial channel pressure was of the order of 5 → 10 millimetres of mercury and the right hand side of equation (4) has been evaluated for a constant pressure of 0.01 ATM (i.e., 7.6 mm mercury).

This assumption enables us to plot a theoretical curve on Fig.7. The agreement with experiment is fair, and the chart should prove a useful guide to the expected signal level ΔV_{JUMP} from a given wall resistance thermometer experiment. It should be noted that at shock Mach numbers above 10, ionisation is present in the hot gas behind the incident shock wave and consequently the signal from the resistance thermometer is affected; 'low' values of ΔV_{JUMP} are occasionally observed. Further details are given in Ref.5.

A similar theoretical curve may be deduced for the value of ΔV_{JUMP} for a stagnation point resistance thermometer. In this case the thermodynamic properties have been evaluated for a stagnation pressure held constant at 10 atmospheres. In this case the theoretical curve agrees very well with the experimental results.

If we return to Fig.6, the magnitude of ΔV_{MAX} cannot be calculated in a simple manner, and here we merely state that for stagnation point work ΔV_{MAX} is up to 5 times ΔV_{JUMP} and for laminar boundary layers $1\frac{1}{2}$ to 2 times ΔV_{JUMP}, whilst for turbulent wall boundary layers ΔV_{MAX} is up to 3 times ΔV_{JUMP}. These experimental values should enable oscilloscope sensitivities to be set up in advance of any desired experiment with reasonable expectation that the vertical deflection will fill the screen. From the results given in Fig.7 we determined that the magnitude of ΔV_{JUMP} was always greater than 5mV (millivolts) except at initial channel pressures less than 0.5 millimetres of mercury. This was additional evidence to support the view that the electronic recording

apparatus was satisfactory in operation. As a further check on this point, a series of runs were made with very low initial channel pressures. The outputs of resistance thermometers under these extreme conditions were displayed on oscilloscopes and photographed. With a diaphragm pressure ratio of 2×10^6, a shock Mach number of 16 was produced when the initial channel pressure was 0.04 mm of mercury and ΔV_{JUMP} was about 2 millivolts. However, it was noted that when ΔV_{JUMP} was below 2 millivolts the operation of the trigger amplifiers became erratic, probably because the input to the thyratron grid is not sufficiently large to ensure very rapid firing of the thyratron.

4.2 Shock speed measurements

In the series of runs from 233 to 620, four calibrated wall type resistance thermometers were placed at stations A_2, B_2, E_2 and F_2 and a further stagnation point type at W_S. In addition, two further wall resistance thermometers were installed at B_1 and F_1, diametrically opposite B_2 and F_2. The outputs of these gauges were displayed on oscilloscopes and photographed in each run. This addition to the data obtained from each run has proved invaluable.

The results of these runs are displayed in Figs. 8, 9, and 10 where the shock speeds over the distances AB, AF and EF respectively are compared with the theoretical value for the experimental diaphragm pressure ratio. The ordinate and abscissa of Figs. 8, 9, and 10 are twice that of the corresponding Figs. 2, 3, and 4 for runs 1 to 232; this emphasises that the scatter in the experimental results has been greatly reduced. Fig.11 compares the shock Mach numbers as measured 13 ft ($M_{S_{AB}}$) and 31 ft ($M_{S_{EF}}$) from the diaphragm; the shock attenuation is clearly shown to be about 10% for all values of shock Mach number. It may be noted in passing that the value of $M_{S_{TH}}$ for the higher shock speeds may be subject to a proportionately greater error than at the lower shock speeds. This is due to difficulties in measuring the initial channel pressure accurately when it is of the order of 0.1 millimetre of mercury.

One criterion which may be applied to the evaluation of the gas dynamic performance of the shock tube will now be described. The measuring intervals AB, AF and EF are 1 foot, 19.125 feet and 1 foot respectively and thus for no shock-wave attenuation the ratios

$$\frac{AF}{AB}, \frac{BE}{AB}, \frac{BE}{EF} \quad \text{and} \quad \frac{AF}{EF}$$

should be 19.125; 17.125, 17.125 and 19.125 respectively. A simple calculation shows that if the speed over AB is the theoretical speed and if we postulate 10% attenuation between AB and EF, then the four ratios above become 20.0, 17.9, 16.2 and 18.1 respectively. If 5% attenuation is the case then the ratios are 19.5, 17.5, 16.6 and 18.6 respectively. As Fig.10 shows, the attenuation observed at a distance 31 feet from the diaphragm is approximately 10%. Thus the majority of all runs in this shock tunnel should exhibit the following feature; the time ratios should be

$$\frac{AF}{AB} > \frac{AF}{EF} \simeq \frac{BE}{AB} > \frac{BE}{EF}.$$

This assumes that the shock attenuation is about 10% and that the shock velocity continuously decreases between AB and EF. The latter point is almost certainly satisfied since Fig.9 shows the velocity over AF is slower than theoretical.

If/

If the attenuation in a given run is greater than 10%

$$\frac{AF}{EF} < \frac{BE}{AB}$$

and if the attenuation is less than 10%

$$\frac{AF}{EF} > \frac{BE}{AB}.$$

Normally $\frac{AF}{EF}$ is approximately equal to $\frac{BE}{AB}$.

This criterion has been applied to all runs after No. 233 and found to be very satisfactory. More than 90% of all runs have time ratios in agreement with the above inequality. Further useful data have been obtained from the wall resistance thermometers B_1 and F_1 mentioned above. As an example of the use of these instruments we may refer to the experimental data collected into Table 1. These are a number of runs made during an investigation of the starting process in the hypersonic nozzle of the shock tunnel. In these experiments a constant shock Mach number at entry to the nozzle was desired; and the pressure ratio P_o across the diaphragm was chosen to give a shock Mach number of 10.0. The variations of P_o from run to run are given in Table 1, and it is seen that the shock velocity over AB is approximately the theoretical value, whilst over EF a 10% attenuation has occurred. The mean values of the results over AB, BE, EF and AF are 87.7, 1706.3, 95.9 and 1888.7, whilst the standard deviations are 1.14, 13.6, 1.32 and 16.7 respectively. The two runs 317 and 322 have been left out of these average values since they do not comply with the time ratio criterion developed above. Moreover, an inspection of the wall resistance thermometer trace at B_1 for run 322 shows that it is very different from that for run 321 - a 'normal' trace*, repeatable from run to run. From records such as these in Fig.12, positive proof can be obtained that the shock tunnel did not function correctly in run 322. It is therefore suggested that any run which does not conform to the time ratio criterion and which also shows irregularities in the wall resistance thermometer traces should be disregarded. Since over 90% of the runs made in the N.P.L. hypersonic shock tunnel are acceptable on this basis, a good degree of confidence can be placed in the shock speed measurements made with our calibrated films (runs 233 onwards). On the other hand, less than 50% of the early runs (up to No.232) are acceptable on the above basis and the results given in Figs. 2, 3 and 4 should be viewed with caution.

Future practice at N.P.L. will be to disregard any run which shows these irregularities in shock speed and wall resistance thermometer traces.

5. Running Time Measurements

We may define the running time of a shock tunnel as the time interval between the passage of the primary shock wave and the passage of the contact surface past a given measuring station along the channel.

Measurements of the running time of the shock tunnel have been made from both wall and stagnation point resistance thermometer records. Details of the detection of the passage of the contact surface from the

observed/

---

*A detailed investigation of the effects of ionisation on the output of thin film resistance thermometers in high enthalpy shock tube flows is to be reported in Ref.5.

observed oscilloscope trace are given in Ref.5; it is found that there is reasonable agreement between the running time as measured from stagnation point records and from the corresponding wall traces. It appears that the most accurate indication is obtained from the stagnation point records. Our results to date are summarised in Figs. 13 and 14. Considerable scatter is to be expected in these results since the contact surface postulated in ideal shock tube theory is actually a mixing region which extends for several tube diameters along the tube. Theoretical calculations of running time using real gas theory[6] are also plotted in Figs. 13 and 14.

Channel pressures above and below 2 millimetres of mercury have been plotted with different symbols; at very low channel pressures there is a shorter running time than that at the same shock Mach number into a pressure of 5 or 10 millimetres of mercury. Fig.15 shows this clearly for two runs with nearly equal shock Mach numbers and channel pressures of 10 and 0.65 millimetres of mercury. The running time decreases catastrophically as the shock Mach number is increased and is only 7 microseconds at a station 13 feet from the main diaphragm at a shock Mach number of 16 into an initial channel pressure of 0.04 millimetres of mercury.

From theoretical considerations the running time 31 feet from the diaphragm should be 31/13 times the running time 13 feet from the diaphragm. An inspection of Figs. 13 and 14 shows that this is not the case and we may analyse the results in the following manner. Firstly, we decided on a 'working curve' of running time as a function of shock Mach number for each measuring station. For obvious reasons we should be conservative in the choice of this curve, so that the 'working value' represents a near minimum value of the expected running time. Normally we would expect to get a slightly greater running time than this 'working value'.

Figs. 13 and 14 show our proposed working curves and the ratio of the running time $\tau_{31 \text{ feet}}$ measured 31 feet from the main diaphragm to the running time $\tau_{13 \text{ feet}}$ measured 13 feet from the main diaphragm has been derived from these working curves. Two separate viewpoints are of interest: firstly the ratio for the <u>same shock Mach number</u> at both measuring stations (and hence different runs due to the shock attenuation) and secondly the ratio for the <u>same run</u> (where $M_{S_{EF}}$ will be about 90% of $M_{S_{AB}}$). These two cases are shown in Figs. 16 and 17 respectively. The results illustrate that the relation between shock attenuation down the channel and the associated variations in available running time is an extremely complicated one and is capable of several interpretations. It appears to the writer that the viewpoint adopted in Fig.16 is the most relevant one; it would therefore seem that there is an optimum length of channel for every shock tunnel. For an increase of channel length beyond the optimum, a small increase of running time would be achieved <u>but</u> this occurs in association with a considerable decrease in shock Mach number due to attenuation.

6. Conclusions

From an analysis of some 600 runs in the N.P.L. hypersonic shock tunnel, a procedure has been devised to ensure that non-repeatable runs with strange features are rejected. It has been found that this shock tunnel can produce extremely repeatable gasdynamic conditions from run to run (as illustrated in Table 1). The use of calibrated wall resistance thermometers as shock trigger timing detectors and as monitor probes to study the flow is strongly recommended and has led to a significant improvement in the quality and reliability of the results from the shock tunnel.

Acknowledgements

Mr. F. S. Pusey and Dr. D. L. Schultz helped in the experimental work and offered helpful suggestions.

References

No.	Author(s)	Title, etc.
1	D. L. Schultz and B. D. Henshall	Hypersonic shock tube equipment at the National Physical Laboratory. NPL/Aero Note/325. May, 1957. A.R.C.19,372
2	D. W. Holder and D. L. Schultz	Notes on the current programme of hypersonic research at the N.P.L. C.C.402. 4th June, 1958.
3	B. D. Henshall and D. L. Schultz	Some notes on the use of resistance thermometers for the measurement of heat transfer rates in shock tubes. C.P.408. May, 1958.
4	H. W. Ladenburg et al W. Bleakney	Physical measurements in gas dynamics and combustion. Vol. IX, High Speed Aerodynamics and Jet Propulsion. Article C5, p.159. Oxford University Press. 1955.
5	B. D. Henshall	The effects of ionisation on the output of thin film resistance thermometers in high enthalpy shock tube flows. (A.R.C. Report in preparation) Jan. 1959.
6	P. H. Rose	Physical Gas Dynamics Research at the AVCO Research Laboratory. AVCO Research Report 9. May, 1957.
7	H. S. Carslaw and J. C. Jaeger	Conduction of heat in solids. Oxford. Clarendon Press, 1947.
8	N. Rott and R. Hartunian	On the heat transfer to the walls of a shock tube. Cornell University Report. November, 1955.
9	D. E. Gray (Ed.)	American Institute of Physics Handbook. McGraw Hill Book Co. Inc. New York. 1957.
10	R. J. Vidal	A resistance thermometer for transient surface temperature measurements. American Rocket Society Paper Buffalo Meeting, September 26, 1956.
11	C. F. Hansen	Approximations for the thermodynamic and transport properties of high temperature air. N.A.C.A. Tech Note 4150. March, 1958.
12	S. Feldman	Hypersonic gasdynamic charts for equilibrium air. AVCO Research Laboratory, Jan. 1957.
13	B. D. Henshall	The theoretical performances of shock tubes designed to produce high shock speeds. A.R.C. C.P.407. May, 1958.

Table 1/

Table 1

Shock Speed Measurements in the N.P.L. Hypersonic Shock Tunnel

Run No.	Diaphragm Pressure Ratio P_o	Time taken by shock between measuring stations			
		AB	BE	EF	AF
		1 foot	$17\frac{1}{8}$ feet	1 foot	$19\frac{1}{8}$ feet
284	6200	86	1695	94	1875
290	6250	87	1698	96	1856
291	6100	86	1715	97	1898
292	6050	88	1708	96	1892
305	6205	86	1685	95	1866
306	6050	87	1698	95	1880
314	6250	87	1716	97	1900
315	6120	88	1723	97	1907
316	6130	88	1715	96	1899
318	5995	88	1704	96	1887
319	6360	87	1700	94	1881
320	6360	87	1673	93	1853
321	6360	87	1695	95	1877
323	6360	88	1698	95	1881
324	6250	89	1710	95	1893
325	6300	89	1719	97	1905
326	6250	88	1707	97	1892
327	6300	88	1697	97	1882
328	6300	88	1716	97	1901
329	6350	89	1709	96	1894
330	6050	89	1735	99	1923
331	6300	89	1727	97	1913
332	6350	87	1702	95	1884
317	6100	75	1871	100	2048
322	6150	64	1661	99	2026

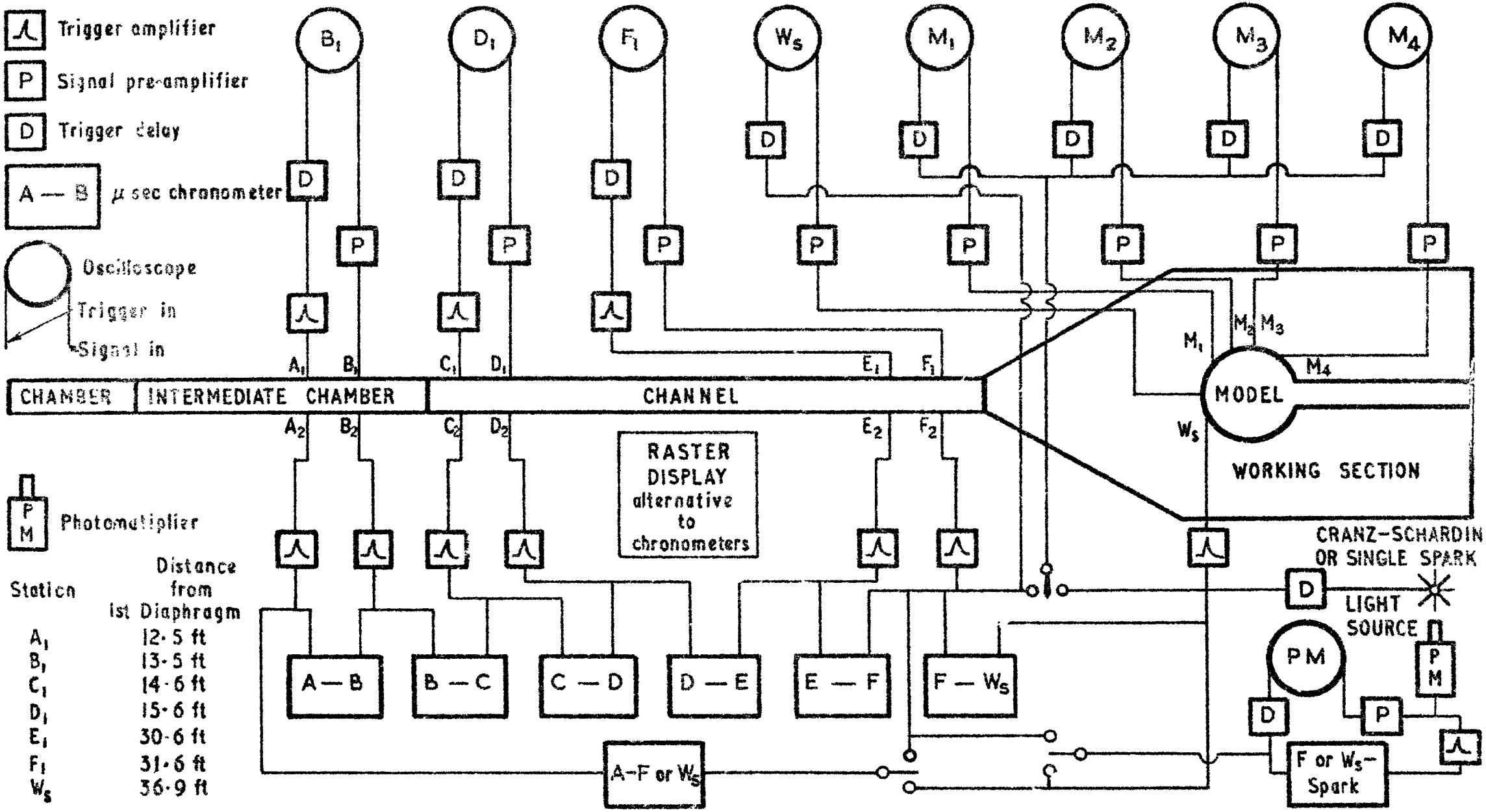

Station	Distance from 1st Diaphragm
A_1	12·5 ft
B_1	13·5 ft
C_1	14·6 ft
D_1	15·6 ft
E_1	30·6 ft
F_1	31·6 ft
W_s	36·9 ft

FIG.1. SCHEMATIC DIAGRAM OF INSTRUMENTATION OF NPL HYPERSONIC SHOCK TUNNEL

Fig. 2.

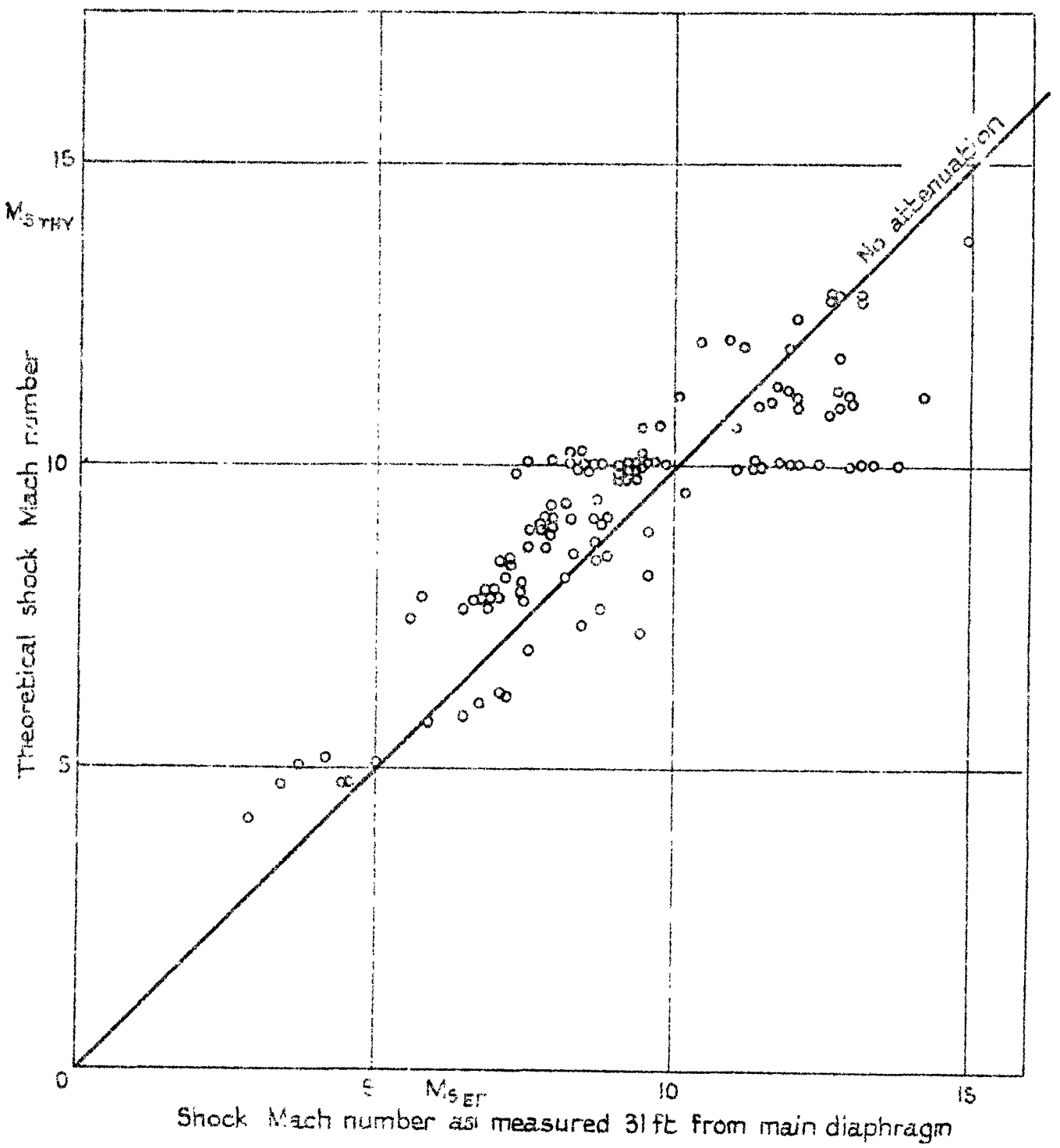

Runs 1 → 232 uncalibrated models

NOL Hypersonic shock tunnel — shock speed measurement

FIG. 3.

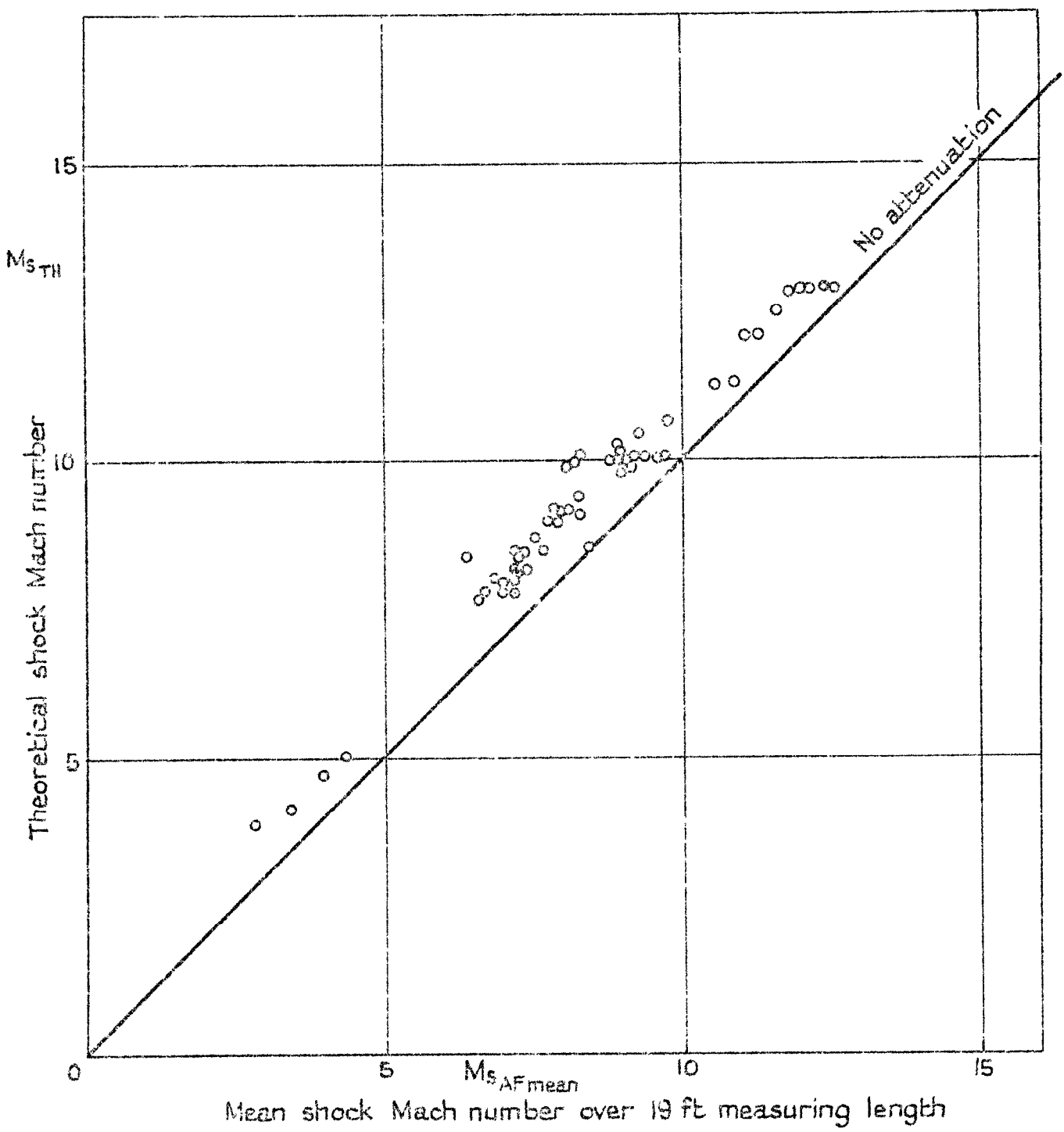

Runs 1 → 232 uncalibrated models

NPL Hypersonic shock tunnel — shock speed measurement

FIG. 4

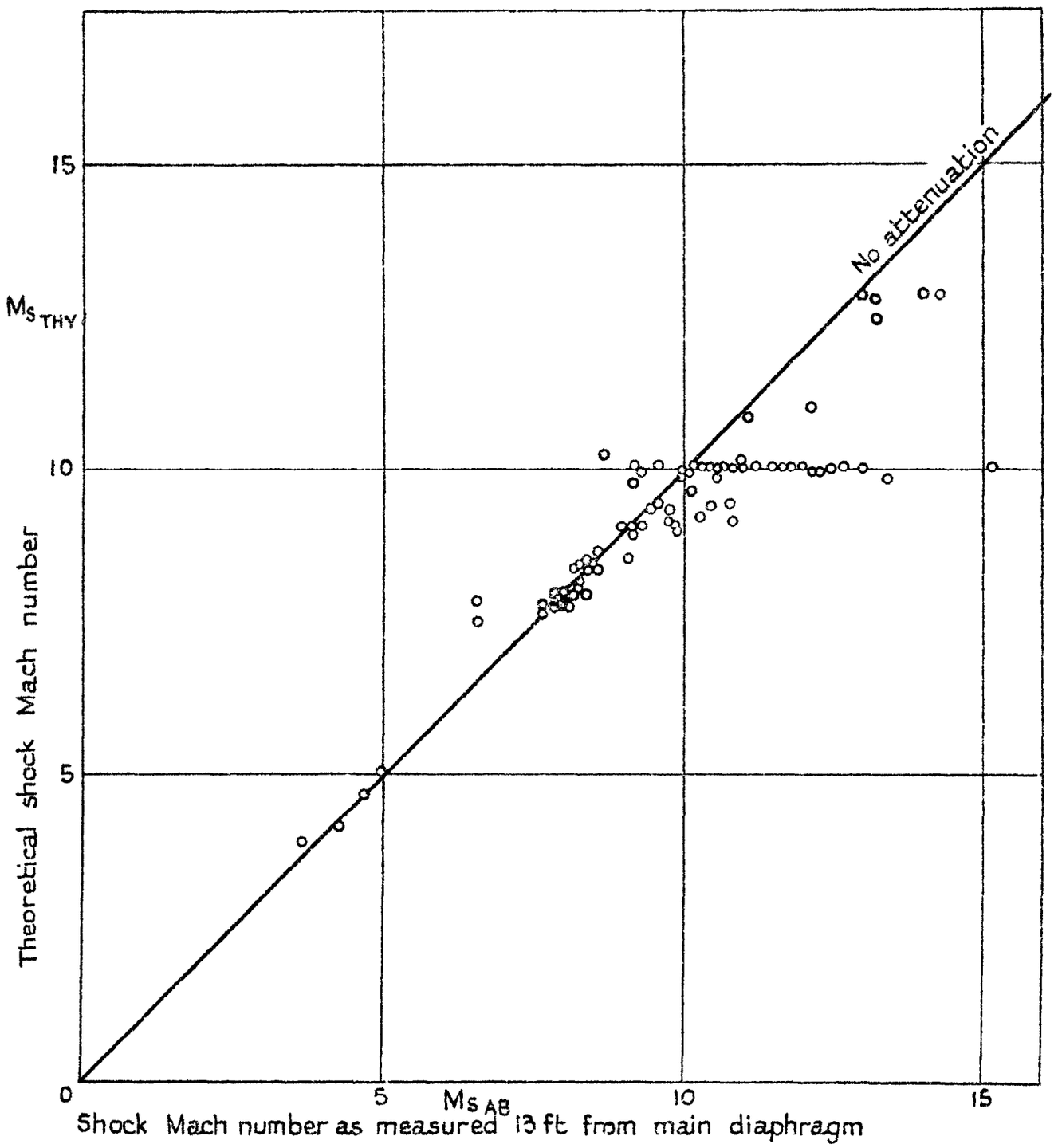

Runs 1→232 uncalibrated models.

NPL Hypersonic shock tunnel—shock speed measurement

FIG. 6.

(a) Sketches of output of resistance thermometers.

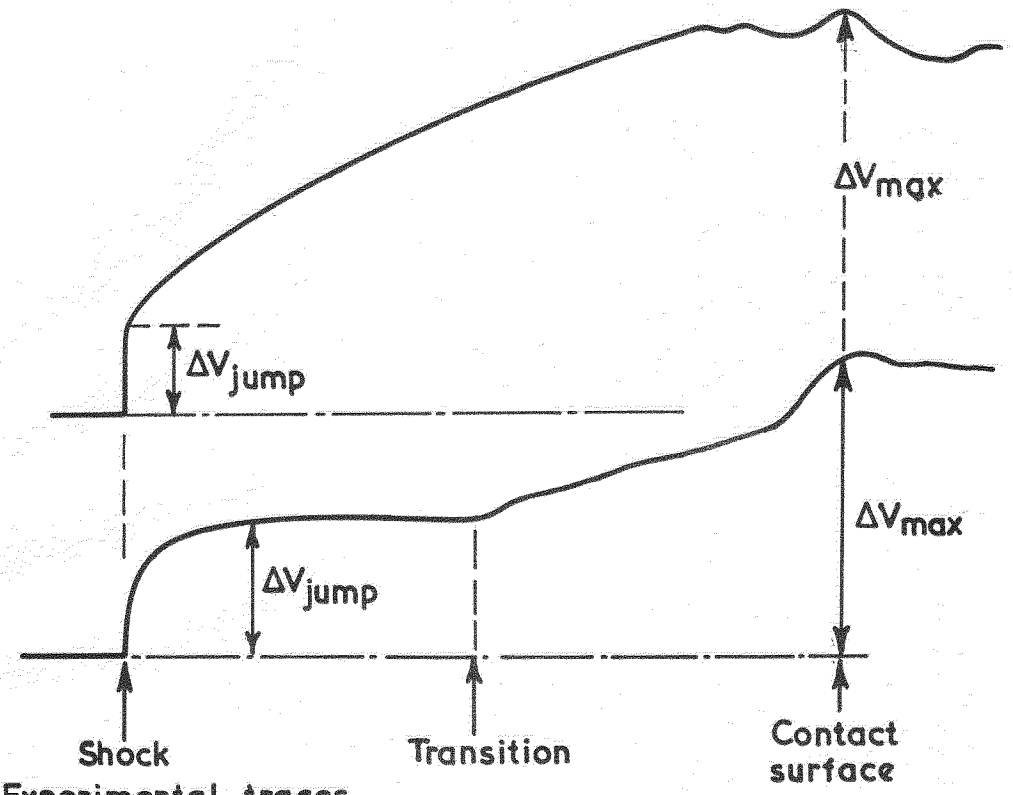

(b) Experimental traces

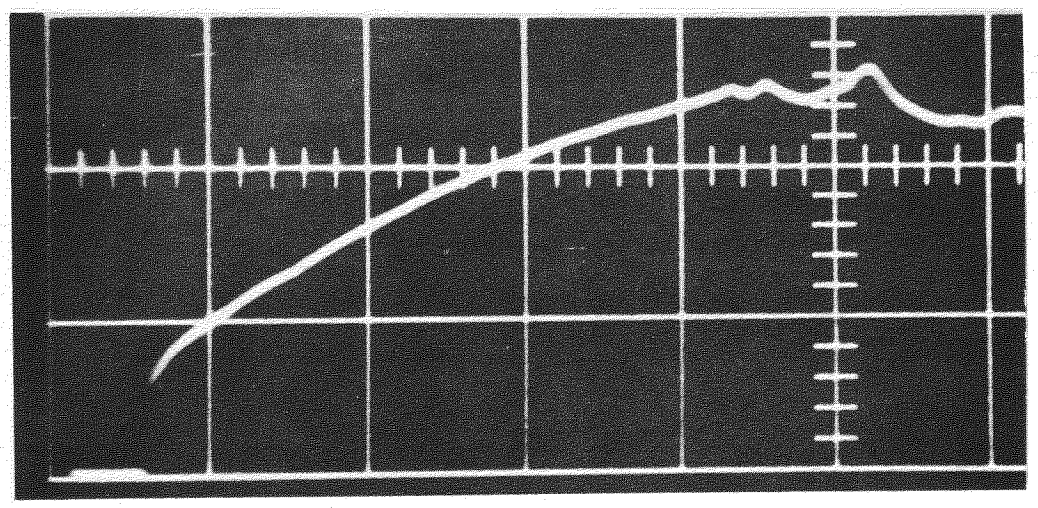

(i) Stagnation point resistance thermometer output

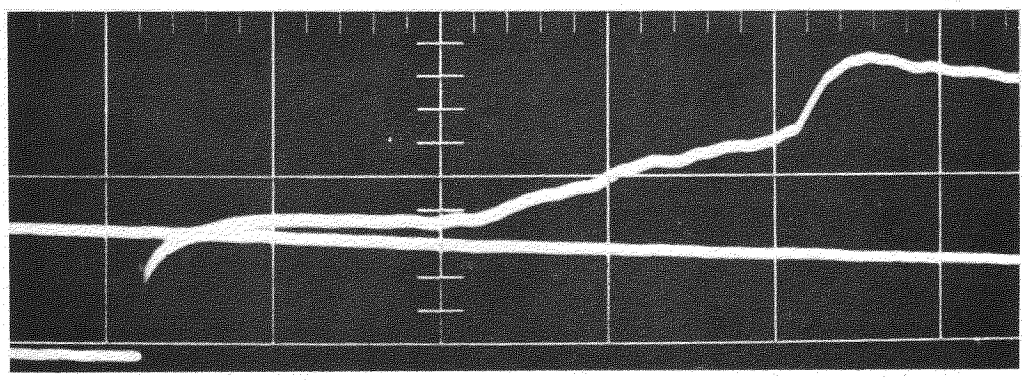

(ii) Wall resistance thermometer output

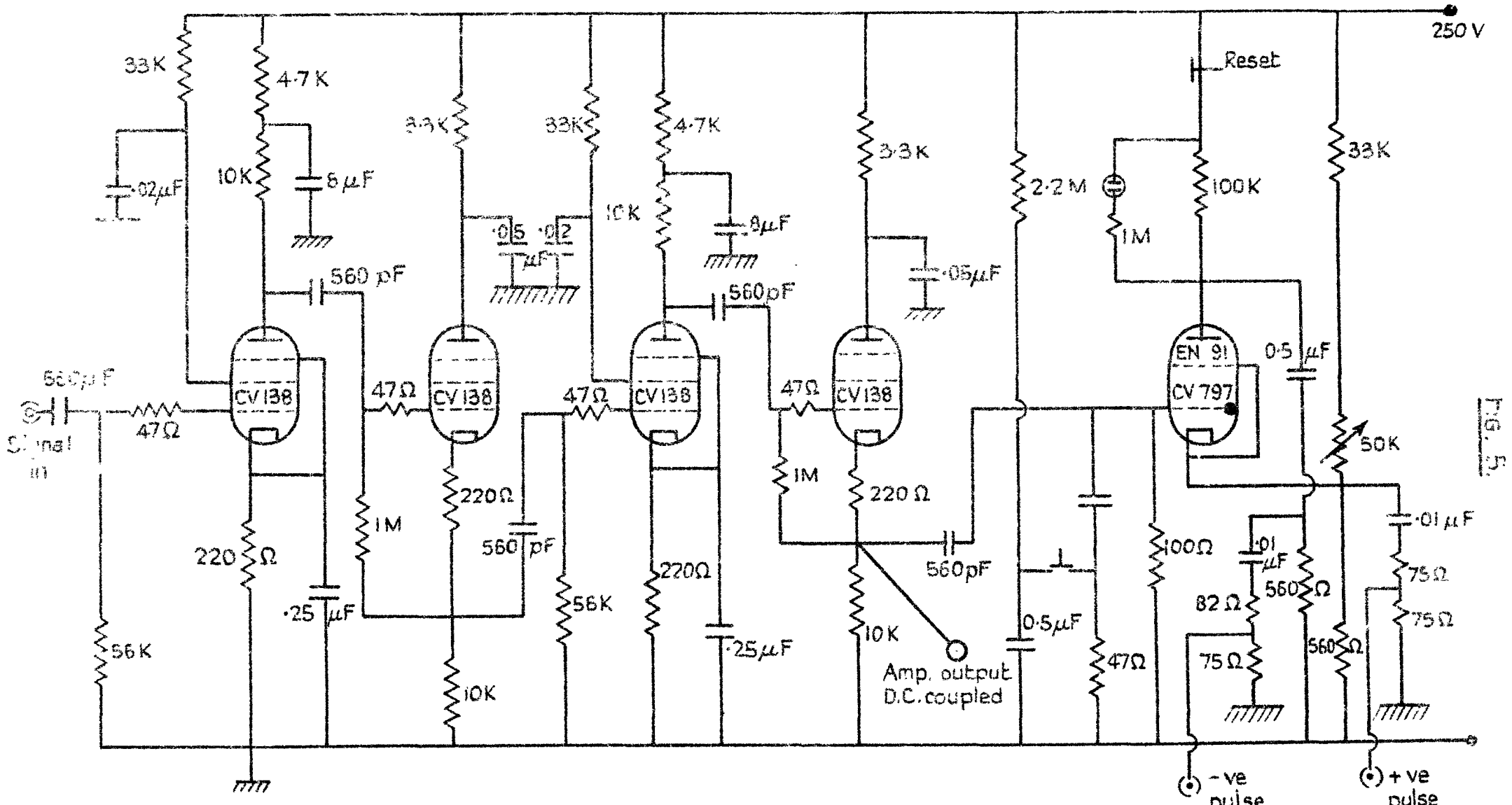

Resistance thermometer trigger amplifier

Fig. 7.

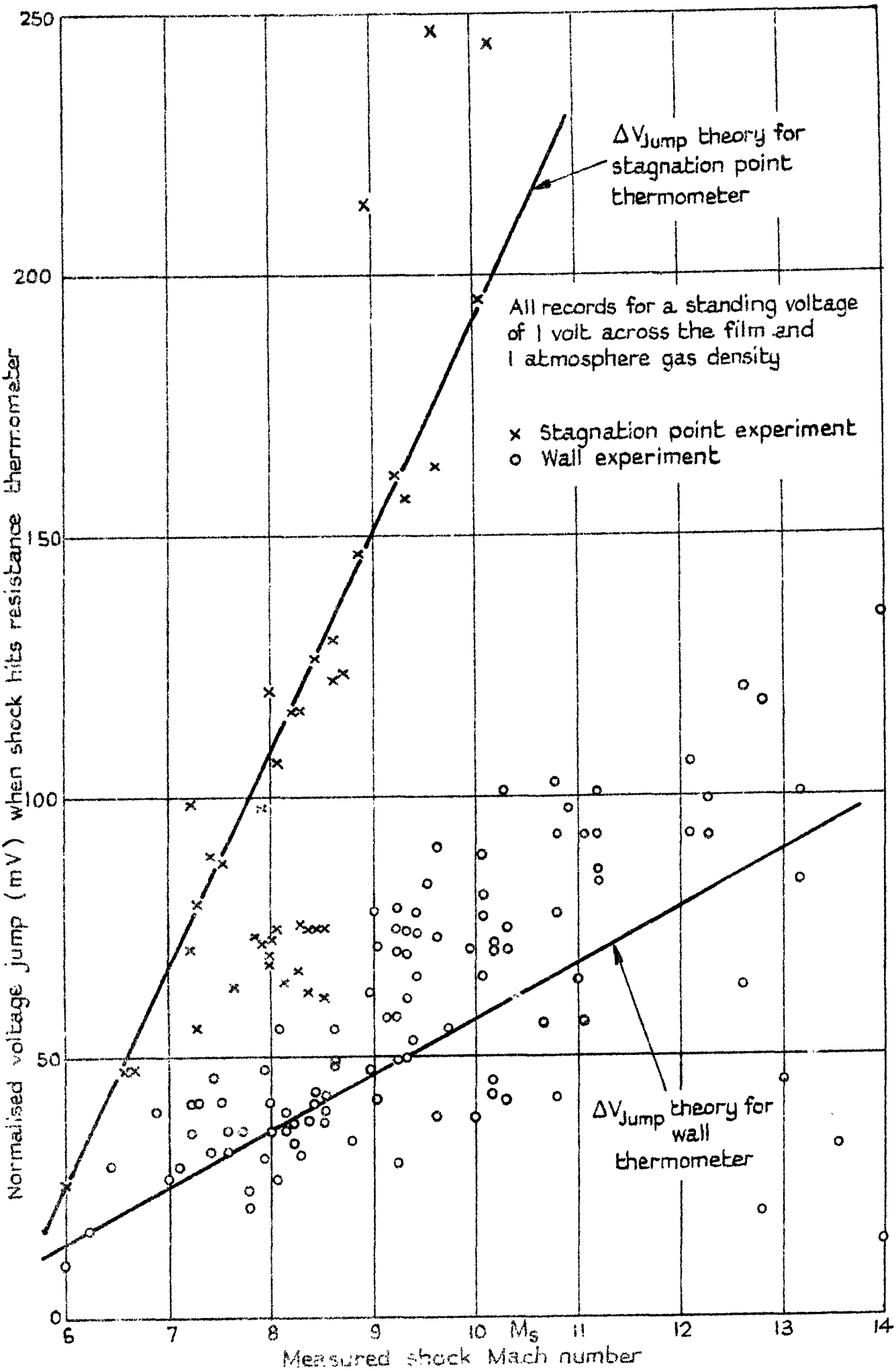

Resistance thermometer outputs:— wall and stagnation point

FIG. 8.

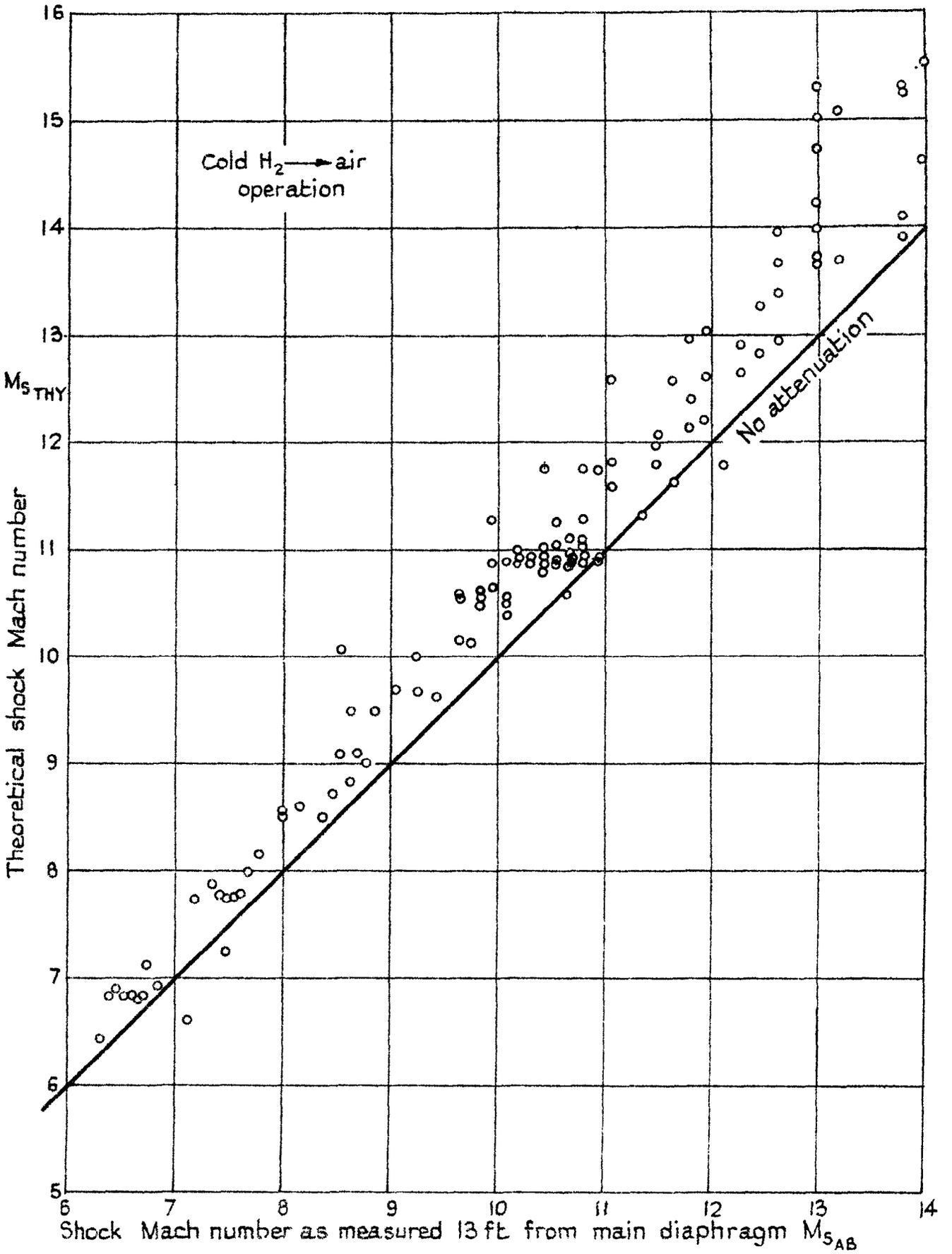

Runs 233 → 620 calibrated models.

NPL hypersonic shock tunnel — shock speed measurements

FIG. 9.

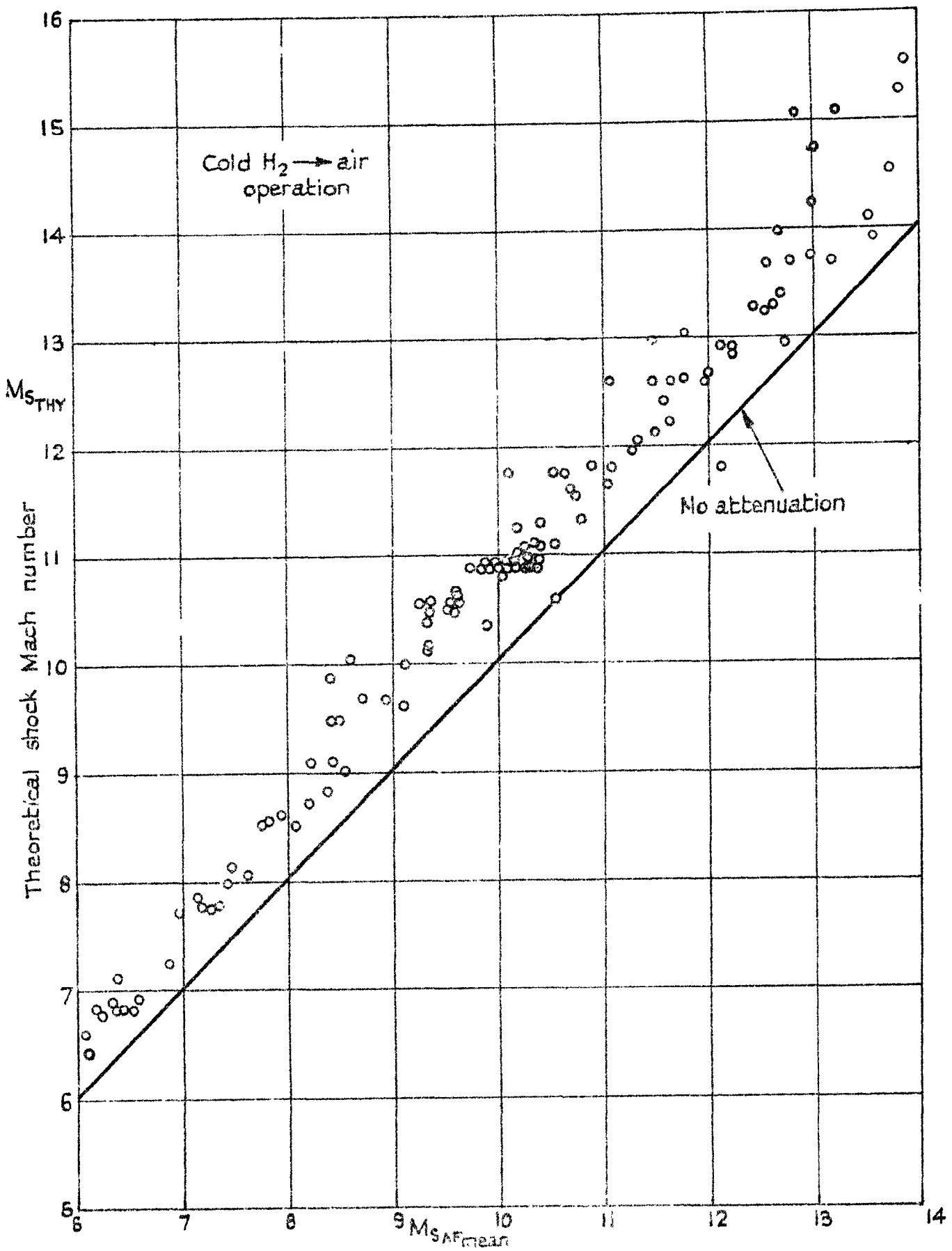

Mean shock Mach number over 19 ft measuring length

Runs 233 → 620 calibrated models.

NPL hypersonic shock tunnel — shock speed measurements

FIG. 10.

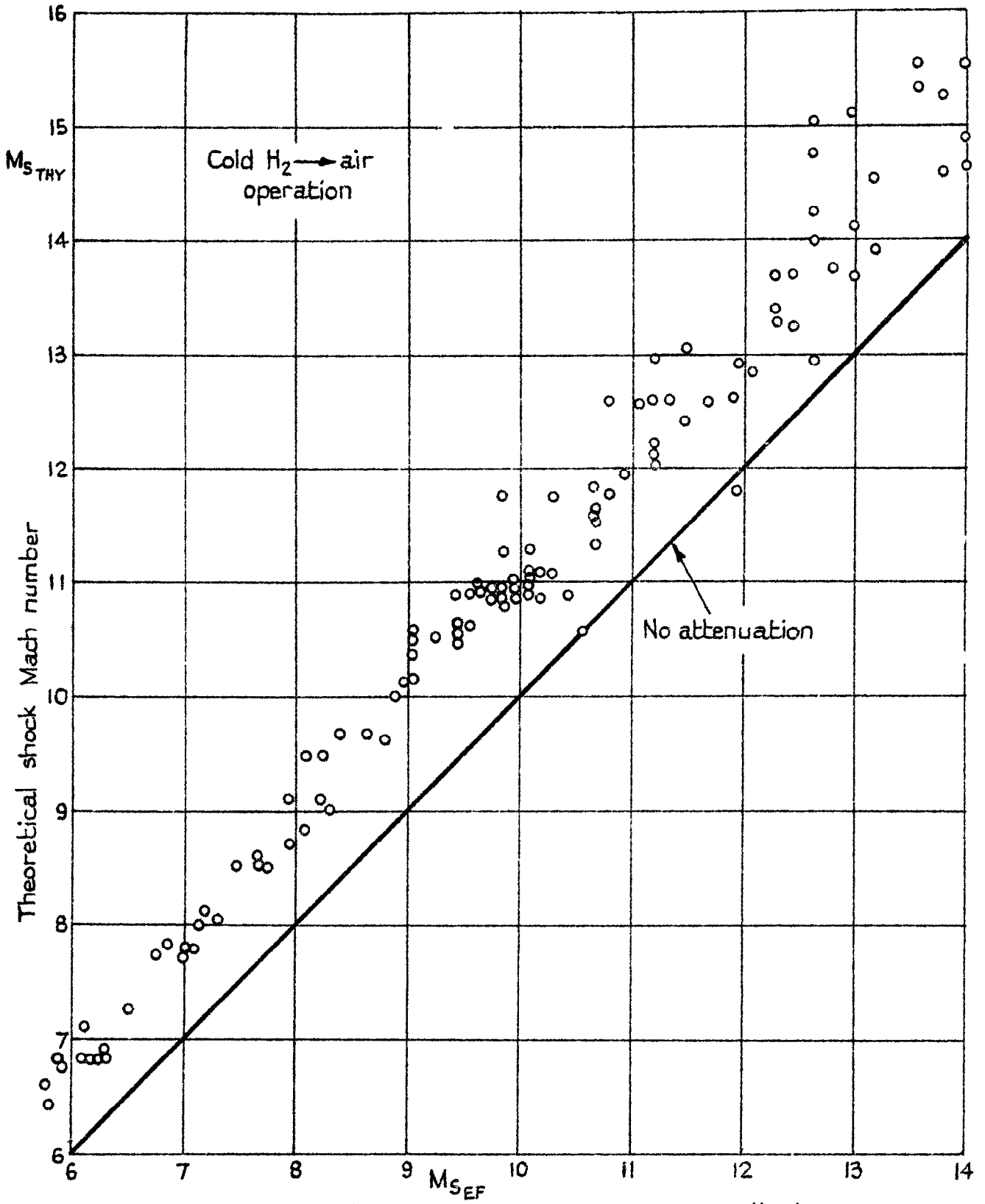

Shock Mach number as measured 31ft from main diaphragm

Runs 233 → 620 calibrated models

NPL hypersonic shock tunnel – shock speed measurements

FIG. 11.

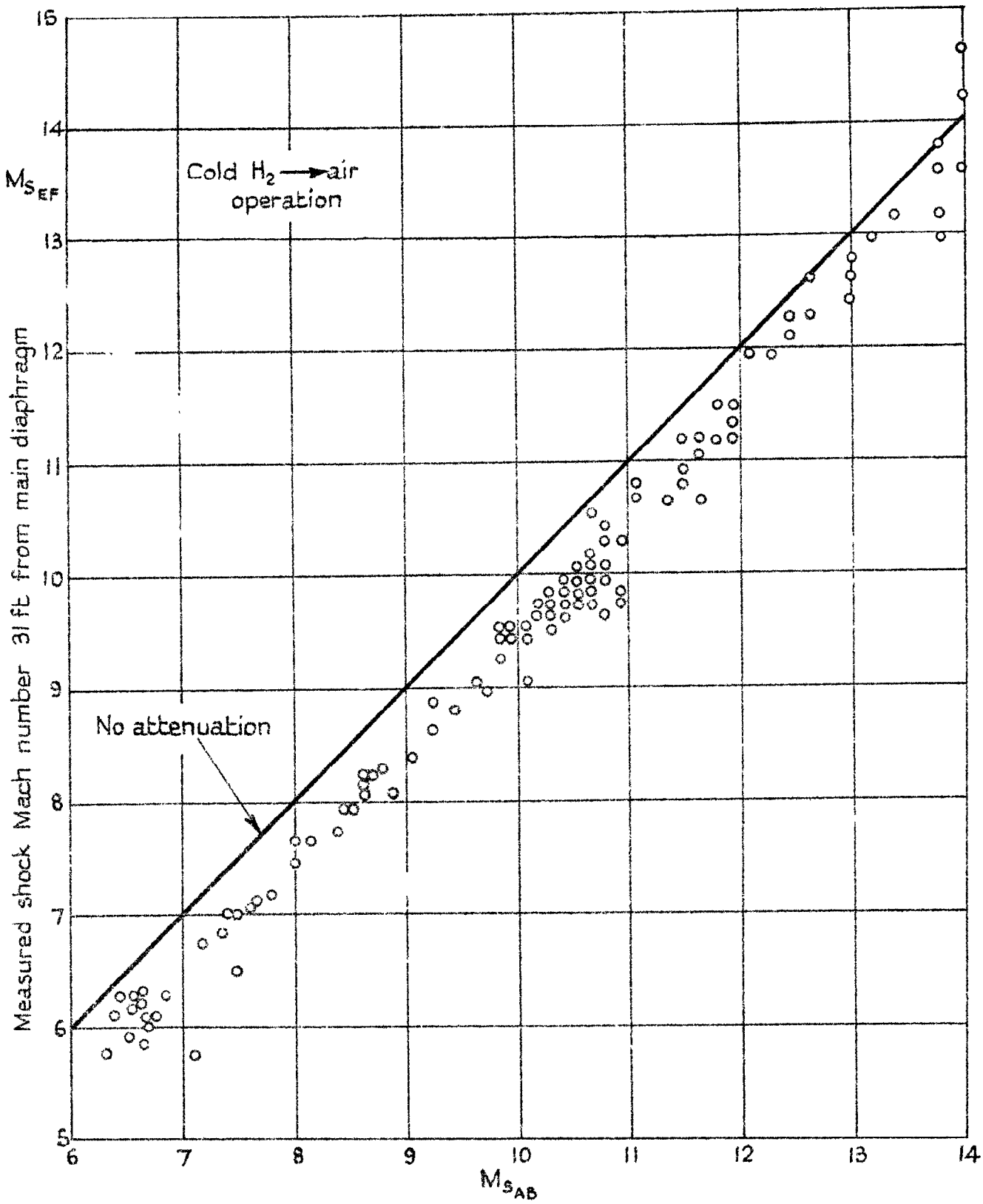

Runs 233 → 620 calibrated models

N P L hypersonic shock tunnel ___ shock speed measurements

FIG. 12.

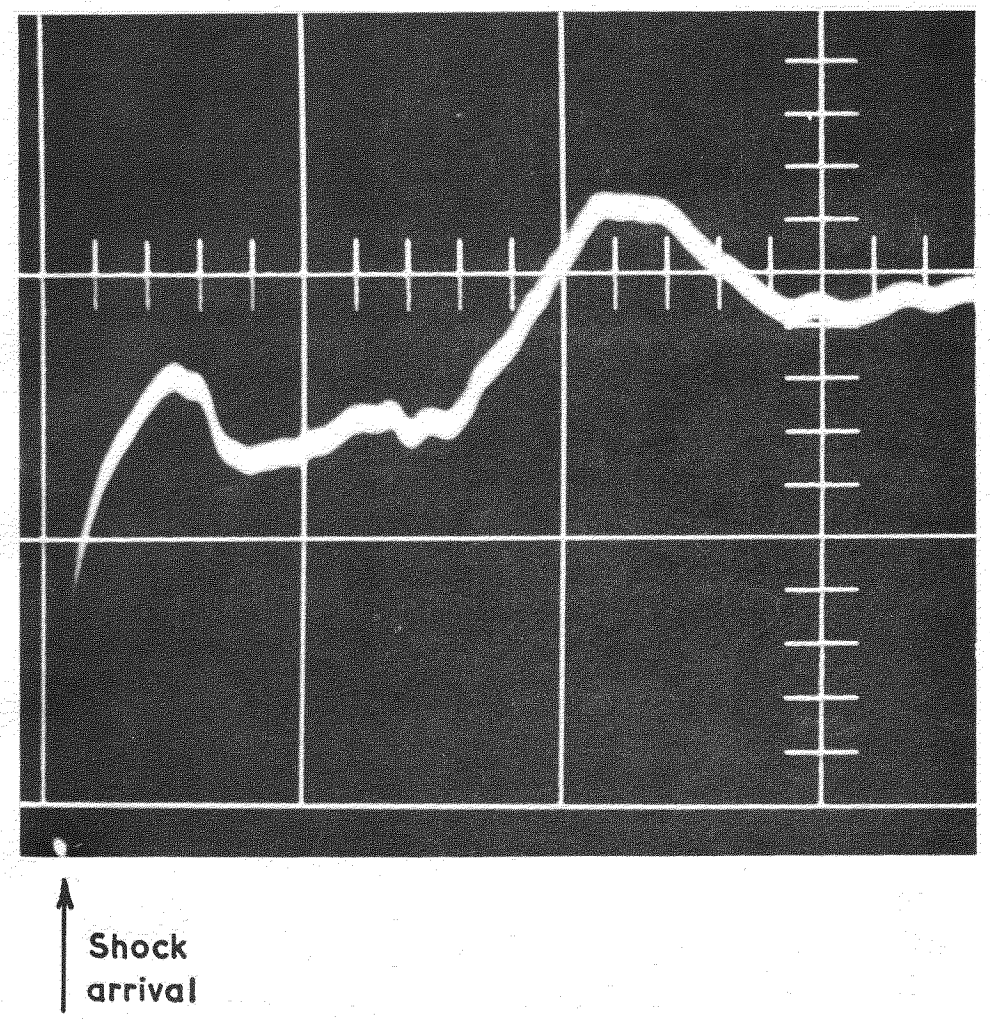

WALL RESISTANCE THERMOMETER TRACES FOR RUNS 321 AND 322
(TO SAME SCALES)

Fig. 13

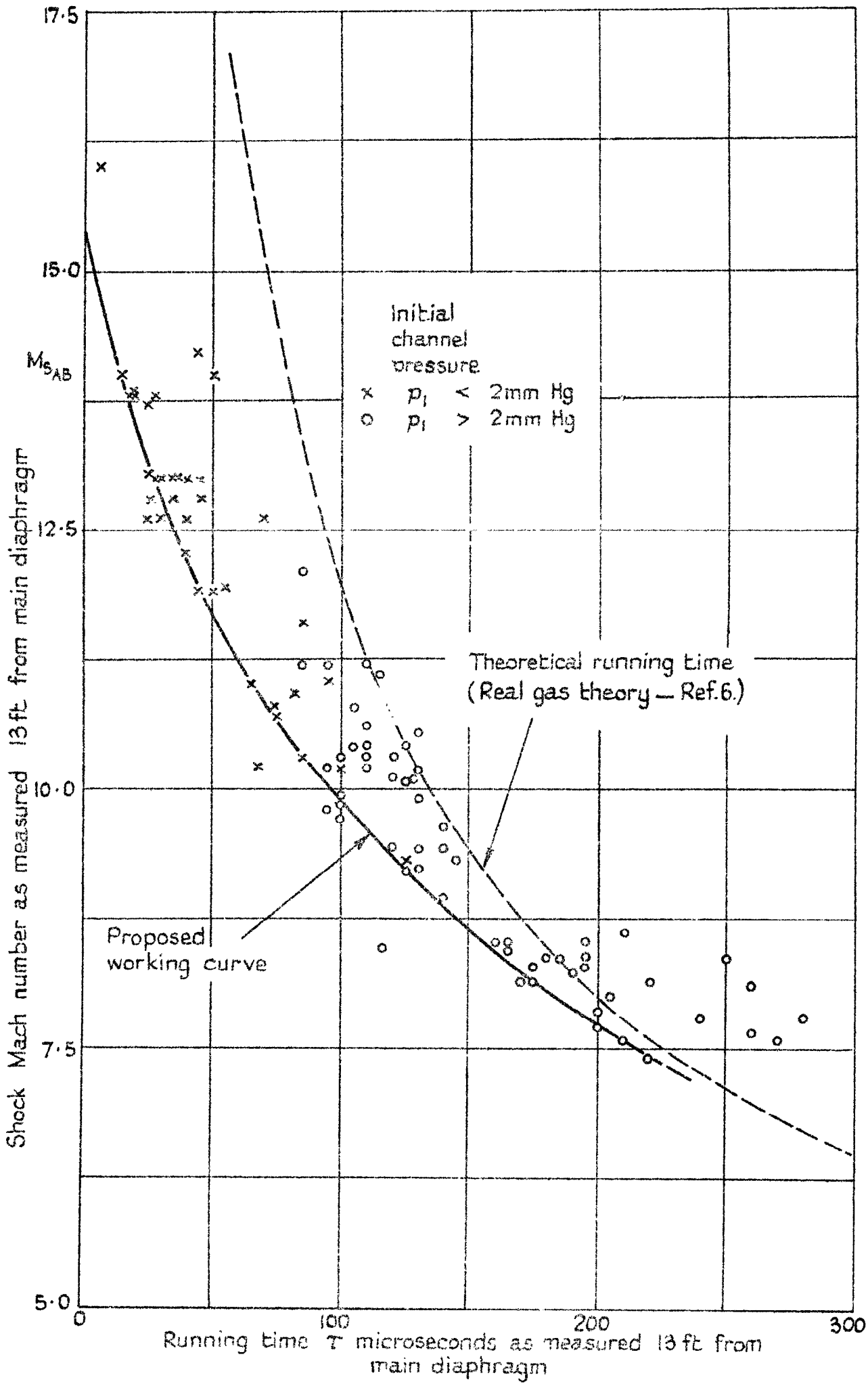

NPL Hypersonic shock tunnel — running time measurements

Fig. 14.

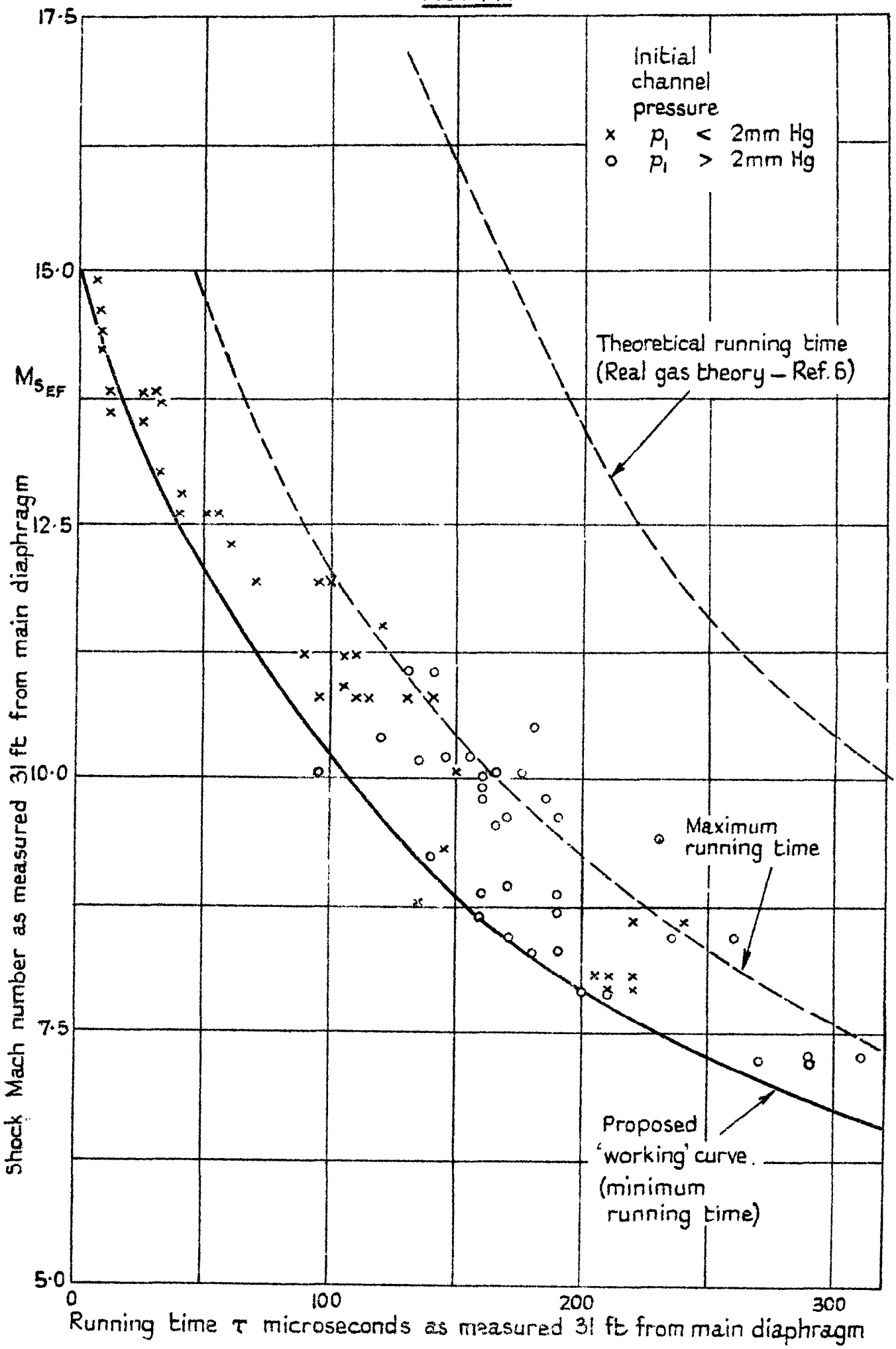

NPL hypersonic shock tunnel – running time measurements

FIG. 15.

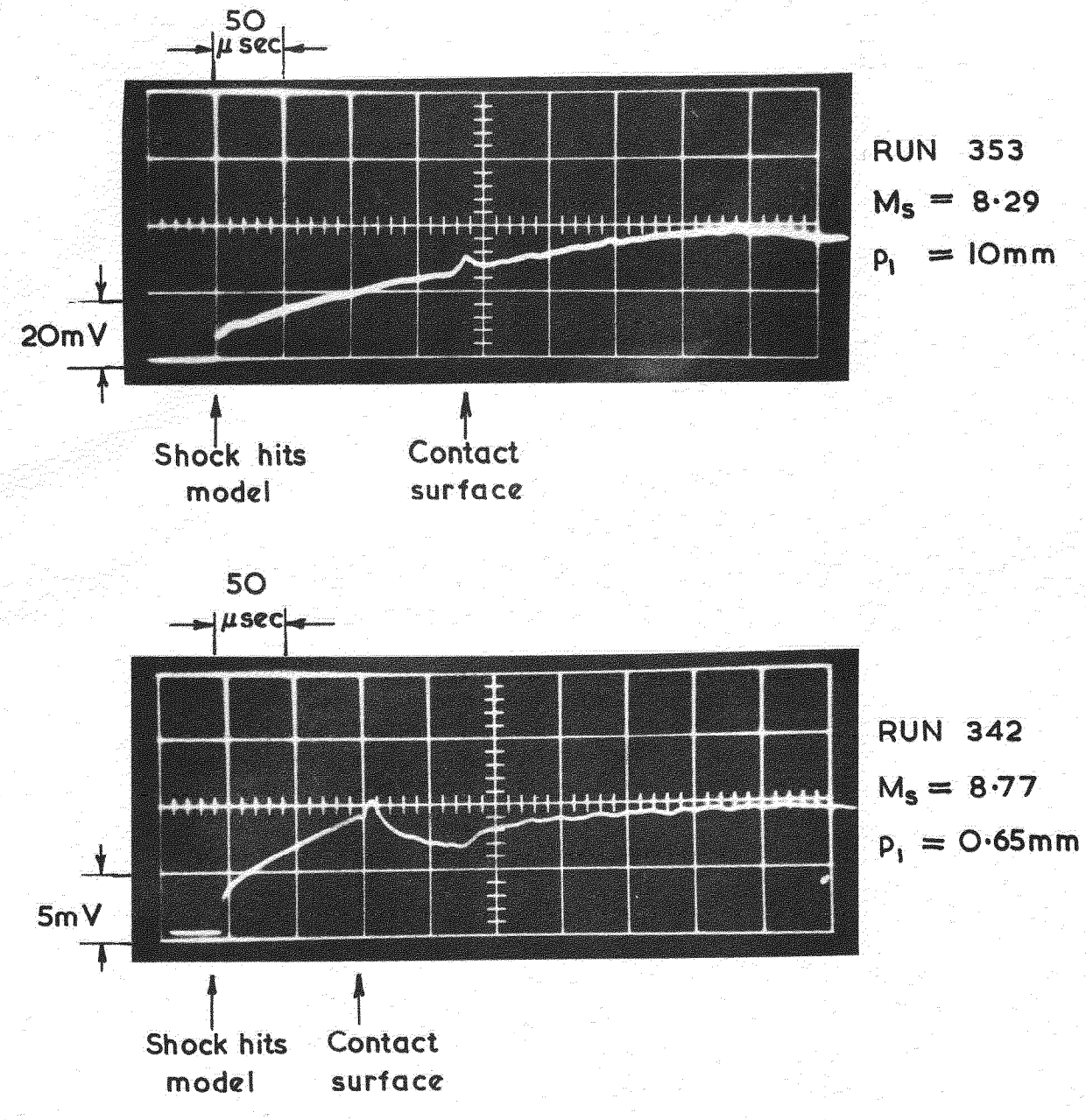

OSCILLOSCOPE TRACES FROM A STAGNATION POINT RESISTANCE THERMOMETER IN THE UNEXPANDED FLOW OF THE NPL HYPERSONIC SHOCK TUNNEL

FIGS. 16 & 17.

FIG. 16.

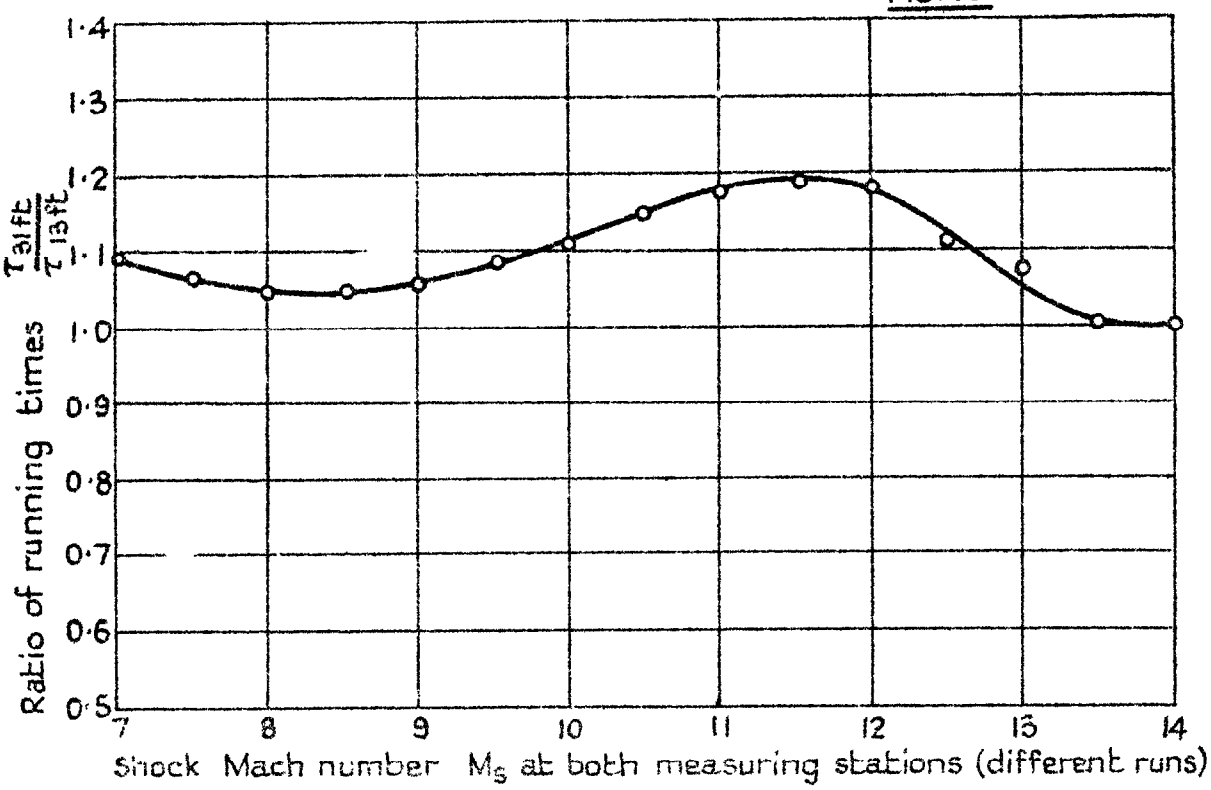

NPL hypersonic shock tunnel — running time measurements.

The ratio of running time measured 31 feet from the main diaphragm to the running time measured 13 feet from the main diaphragm for the same shock Mach number

FIG. 17

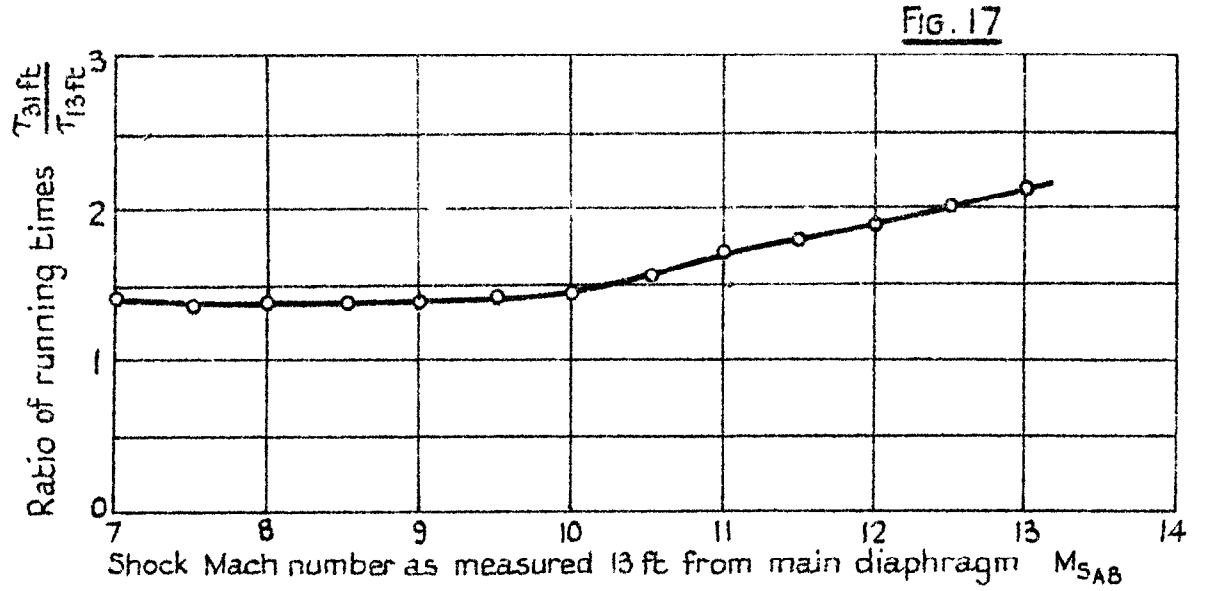

NPL. hypersonic shock tunnel - running time measurements.

The ratio of running time measured 31 feet from the main diaphragm to the running time measured 13 feet from the main diaphragm to the same run (i.e. $M_{S_{EF}} \sim 90\%$ of $M_{S_{AB}}$)

C.P. No. 443
(20,720)
A.R.C. Technical Report

Printed and published by
HER MAJESTY'S STATIONERY OFFICE

To be purchased from
York House, Kingsway, London W.C.2
423 Oxford Street, London W.1
13A Castle Street, Edinburgh 2
109 St Mary Street, Cardiff
39 King Street, Manchester 2
Tower Lane, Bristol 1
2 Edmund Street, Birmingham 3
80 Chichester Street, Belfast
or through any bookseller

Printed in Great Britain

S.O. Code No. 23-9011-43

C.P. No. 443